A novel multifunctional role for Hsp70 in binding post-translational modifications on client proteins

Nitika[1*], Bo Zheng[1], Linhao Ruan[2,3], Jake T. Kline[6], Jacek Sikora[7], Mara Texeira Torres[8], Yuhao Wang[2,3], Jade E. Takakuwa[1] Romain Huguet[9], Cinzia Klemm[8], Verónica A. Segarra[10], Matthew J. Winters[11], Peter M. Pryciak[11], Peter H. Thorpe[9], Kazuo Tatebayashi[12,13], Rong Li[2,3,4,5], Luca Fornelli[6] and Andrew W. Truman[1]*

Author Affiliations

[1]Department of Biological Sciences, The University of North Carolina at Charlotte, Charlotte, NC 28223 USA
[2]Center for Cell Dynamics and Department of Cell Biology, Johns Hopkins University School of Medicine, Baltimore, MD 21205 USA.
[3]Biochemistry, Cellular and Molecular Biology (BCMB) Graduate Program, Johns Hopkins University School of Medicine, Baltimore, MD 21287 USA.
[4]Mechanobiology Institute and Department of Biological Sciences, National University of Singapore, Singapore 117411
[5]Department of Chemical and Biomolecular Engineering, Whiting School of Engineering, Johns Hopkins University, Baltimore, MD 21218 USA.
[6]Department of Biology, University of Oklahoma, Norman, OK 73019 USA
[7]AbbVie Inc., La Grange, IL 60525 USA
[8]School of Biological and Chemical Sciences, Queen Mary University, London E1 4NS UK
[9]Thermo Scientific, San Jose, CA 95134 USA
[10]Department of Biology, High Point University, High Point, NC 27268 USA
[11]Department of Biochemistry and Molecular Pharmacology, University of Massachusetts Medical School, Worcester, MA 01605 USA
[12]Laboratory of Molecular Genetics, Frontier Research Unit, Institute of Medical Science, The University of Tokyo 108-8639, Tokyo, Japan
[13]Department of Biological Sciences, Graduate School of Science, The University of Tokyo, Tokyo 113-0033, Japan
*Correspondence: nnitika@uncc.edu (N), atruman1@uncc.edu (A.W.T.)
ORCID: https://orcid.org/0000-0002-6409-3723

Running title

Hsp70 XL-MS interactome reveals new roles in PTM binding

Abbreviations: AP-MS, Affinity purification mass spectrometry; BiFC, Bimolecular fluorescence complementation; CMV, human cytomegalovirus promoter; CTD, C-terminal Domain; DSSO, disuccinimidyl sulfoxide; GO, Gene ontology; HSE, Heat Shock Response Element; HSP, Heat Shock Protein; MS, mass spectrometry; NBD, Nucleotide-binding domain; PTM Post-translational modifications; SBD, Substrate-binding domain; VN, Venus amino-terminal end, VC, Venus carboxy-terminal end; XL-MS, Cross-linking mass spectrometry; Y2H, Yeast two-hybrid

- *In vivo* confirmation of Hsp70 dimerization
- Comprehensive direct interactome of Hsp70
- Multi-domain interactions between Hsp70 and client proteins
- Identification of novel biologically-important client protein PTMs

Summary

Hsp70 interactions are critical for cellular viability and the response to stress. Previous attempts to characterize Hsp70 interactions have been limited by their transient nature and inability of current technologies to distinguish direct vs bridged interactions. We report the novel use of cross-linking mass spectrometry (XL-MS) to comprehensively characterize the budding yeast Hsp70 protein interactome. Using this approach, we have gained fundamental new insights into Hsp70 function, including definitive evidence of Hsp70 self-association as well as multi-point interaction with its client proteins. In addition to identifying a novel set of direct Hsp70 interactors which can be used to probe

chaperone function in cells, we have also identified a suite of PTM-associated Hsp70 interactions. The majority of these PTMs have not been previously reported and appear to be critical in the regulation of client protein function. These data indicate that one of the mechanisms by which PTMs contribute to protein function is by facilitating interaction with chaperones. Taken together, we propose that XL-MS analysis of chaperone complexes may be used as a unique way to identify biologically-important PTMs on client proteins.

Keywords: Hsp70, Ssa1, chaperone, cross-linking, mass spectrometry, post-translational modifications, interactions, proteomics

Introduction

The maintenance of a correctly folded proteome (proteostasis) is critical for cell survival. Cells maintain proteostasis under both basal and stress conditions through the expression of folding chaperones such as Hsp70 and its associated co-chaperone regulators (Hartl et al., 2011; Rosenzweig et al., 2019a). Hsp70 function is dependent on three conserved domains: an N-terminal nucleotide binding domain (NBD), a substrate ("client")-binding domain (SBD), and a C-terminal ("lid") domain (Frydman et al., 1994; Radons, 2016). The binding and hydrolysis of ATP to ADP in the NBD promotes large-scale structural Hsp70 rearrangements that allow the closing of the CTD over client proteins that bind in the SBD, promoting protein folding (Chirico et al., 1998; Rosenzweig et al., 2019b). The characterized roles of Hsp70 include folding of new and denatured proteins; transport of mitochondrial proteins and disaggregation of protein complexes (Artigues et al., 2002; Bush and Meyer, 1996; Nitika and Truman, 2017).

The essential nature of Hsp70 function in the cell, as well as its involvement in a variety of human pathologies such as cancer, has driven researchers to set out to characterize Hsp70 interactors. While great strides have been made towards this goal, these efforts have been hampered by limitations in the technologies used. For example, these past efforts have utilized affinity purification followed by mass spectrometry (AP-MS), yeast two-hybrid (Y2H) and proximity proteomics methodologies, all of which lack the ability to discriminate between direct and bridged protein interactions (Gentzel et al., 2019; Millson et al., 2005; Truman et al., 2015; Vidal et al., 1996; Zhao et al., 2005). Chemical cross-linking with mass spectrometry (XL-MS) is a powerful interactomic technique that circumvents this issue, providing information on direct interactions in protein complexes by using chemical cross-linkers (Leitner et al., 2016; Liu et al., 2015). Indeed, XL-MS studies are often complementary to the traditional structural biology methods such as X-ray crystallography, nuclear magnetic resonance, and cryo-electron microscopy (Liu et al., 2015).

Importantly, a key role for Hsp70 function is stabilization and activation of a wide range of signaling molecules including those involved in processes such as DNA damage response, cell cycle control, autophagy and nutrient sensing (Dubrez et al., 2019; Gupta et al., 2018; Truman et al., 2012; Yang et al., 2013). The Hsp70 client proteins involved in these cellular processes tend to be either highly post-translationally modified (PTMs) or regulate PTMs on other proteins. In turn, these PTMs tightly regulate a multitude of protein properties including subcellular localization, enzymatic activity and protein interactions (Nitika et al., 2020). Advances in mass spectrometry-based methods have allowed identification of more than 200 different types of PTMs on proteins including

phosphorylation, acetylation, and ubiquitination (Beltrao et al., 2012; Catherman et al., 2014; Dushukyan et al., 2017). Given the numerous PTMs identified on proteins, researchers are now facing difficult choices when selecting specific PTMs for further study. Computational methods for identifying important PTMs on proteins have been partially successful but rely on pre-existing MS data (Beltrao et al., 2012; Swaney et al., 2013). In this report, we have utilized XL-MS to comprehensively understand the Hsp70 interactome. In doing so, we have uncovered not only a new set of Hsp70 client proteins, but show that these clients bind at multiple sites on Hsp70, including the N-terminal NBD. Notably, many of the Hsp70 interactions with client proteins are in close proximity to biologically-important PTMs. All in all, our data suggest that our XL-MS approach to chaperone interactome characterization can also be used as a novel way to identify biologically-important and previously unknown PTMs on client proteins.

Results

Analysis of cross-linked yeast Hsp70 complexes

Previous studies have identified proteins in complex with yeast Hsp70 (Ssa1) using quantitative AP-MS (Truman et al., 2015). To comprehensively identify direct Ssa1 client proteins and associated surfaces of interaction, we took a novel cross-linking proteomics approach. HIS-tagged Ssa1 was expressed in *ssa1-4*Δ, a yeast strain in which all four *SSA* (Hsp70) genes have been deleted. HIS-Ssa1 complexes, with or without cross-linking with disuccinimidyl sulfoxide (DSSO), were characterized via mass spectrometry (Figure 1A). This approach facilitated the characterization of Ssa1 complexes without competition from other native Hsp70 isoforms. Quantitative proteomics identified 1,510

interactors associated with HIS-Ssa1 in the cross-linked complexes and 1,152 in the HIS-Ssa1 complexes without DSSO-mediated cross-linking (Figure 1B). We anticipated that proteins present in the DSSO-treated complexes may consist of direct Ssa1 interactors including client proteins and co-chaperones. To distinguish direct interactors of Ssa1 from indirect interactors, we filtered our data for cross-linked peptides where at least one of the identified peptides was Ssa1. We identified a total of 363 Ssa1-containing cross-linked peptides, out of which 177 were Ssa1-client/co-chaperone crosslinks and 106 were Ssa1-Ssa1 cross-links (Figure 1C). Validating our methodology, no cross-linked peptides were observed in the control uncross-linked sample. To determine whether the cross-linking process had enriched for any particular class of protein, we performed Gene Ontology (GO) analysis of unique candidate interactors of cross-linked and control samples. This GO analysis revealed enrichment of multiple cellular functions (Figure 1D). In the cross-linked samples, proteins involved in protein folding, trafficking and cell signaling were all enriched, synergistic with the established roles of Hsp70.

Dimerization of Ssa1 is required for a subset of chaperone functions

Nearly a third of the cross-linked peptides detected in our experiment were between two Ssa1 peptides (Figure 1C). To distinguish whether the cross-linked Ssa1-Ssa1 peptides came from dimerized Ssa1 molecules as opposed to single intramolecular cross-links, we initially mapped the identified cross-links onto homology-based Ssa1 models. Given the large conformational change Hsp70 undergoes during its folding cycle, we utilized two models, an ADP-bound closed structure and an ATP-bound open structure model (Figure 2A and B). The mapping of cross-links onto these models revealed that a substantial

number of Ssa1-Ssa1 peptides had cross-linking lengths well within the spacer arm limit for DSSO (Figure 2B), while many others exceeded the lengths possible by cross-linking within a single molecule, implying dimerization. Considering that both bacterial and mammalian Hsp70 dimerize, we evaluated whether these cross-links provided evidence for yeast Hsp70 (Ssa1) dimerization. After mapping Ssa1-Ssa1 cross-linked peptides onto a possible Ssa1 dimer structure model based on PDB structure 2KHO (Figure 2C), it was evident that at least a subpopulation of Ssa1 dimerizes in yeast (Figure 2C and 2D). To confirm this, we expressed both FLAG- and HA-tagged Ssa1 constructs in yeast. After immunoprecipitation of FLAG-Ssa1, the interaction between both tagged forms was observed (Figure 2E). Although self-interaction of yeast Hsp70 has been previously observed *in vitro* (Sarbeng et al., 2015), it has never been detected in live cells. To visualize Ssa1-Ssa1 interaction *in vivo*, we utilized bimolecular fluorescence complementation (BiFC). Yeast expressing Ssa1 tagged with Venus amino-terminal end (VN) and Venus carboxy-terminal end (VC) were examined using high-resolution fluorescence microscopy. Imaging of these cells revealed that Ssa1 dimers were clearly visible and that they localized primarily to the nucleus (Figure 2F). To demonstrate *in vivo* functionality of the Ssa1 dimer, residues identified as being present on the dimer interface based on the DnaK model (PDB: 4JNE) —E540 and N537—were mutated to A and K, respectively, generating a dimer-deficient mutant (Sarbeng et al., 2015). While yeast cells expressing the E540A/N537K dimer-deficient mutant were viable and grew at approximately WT rates, they were impaired for growth at high temperature (Figure 2G). To further explain this temperature-sensitive phenotype, we assessed the Heat Shock Response Element (HSE)-luciferase activity in WT and Ssa1 dimer-deficient cells. WT

cells produced a robust HSE-luciferase signal after heat exposure and dimer-deficient cells did not (Figure 2H). Because Ssa1 is a major hub for protein folding in yeast, we set out to examine the possibility that some of the observed Ssa1-Ssa1 interactions might be the result of active Ssa1 folding a newly synthesized Ssa1 polypeptide chain. We studied the interactions of FLAG-Ssa1 (WT and substrate-binding deficient mutant V435F) with a known client, Rnr2 (Truman et al., 2015), the Ydj1 co-chaperone, and HA-Ssa1. Although WT Ssa1 co-purified with Rnr2, Ydj1 and Ssa1, the V435F mutant maintained interaction with Ydj1 and Ssa1, demonstrating that Ssa1 is not a client of other Ssa1 molecules (Figure 2I). Taken together, these findings confirm that Ssa1 dimerizes in yeast and that this self-interaction is important for a subset of Ssa1 functions.

Hsp70 interacts with clients throughout its domains

Our Hsp70 cross-linking strategy identified 124 new direct interactors of Ssa1 (Table S1). Unique direct binding proteins identified using XL-MS were mapped on the domain structure of Hsp70 (Figure 3A). We detected interactions on 58% of the DSSO-accessible lysines (Figure 3A). Interestingly, in contrast to the established paradigm that Hsp70 client proteins bind and interact solely at the SBD, the majority (79%) of the identified direct interactions mapped to the NBD (Figure 3A). Given that DSSO cross-links lysines, we considered that an explanation for such a high number of interactions with the Ssa1 NBD may be explained by the number and distribution of lysines present in each domain. Even when accounting for the relatively large number of cross-linkable lysines, the NBD bound over six times the number clients per cross-linkable lysine compared to the SBD (Figure S1B and S1C). While many of the NBD direct interactors relate to expected cell processes such as translation, chromatin organization and protein folding, there are several with

unknown biological functions (Figure 3B). To validate our XL-MS screen, we confirmed several of our hits using co-immunoprecipitation and immunoblotting. Consistent with our MS data, Cct8, Pcl7, Ura8 and Sse1 all co-purified with Ssa1 and associated chaperones/co-chaperones Sse1, Hsp82 and Ydj1 (Figure 3C).

Exploring the biological importance of novel XL-MS-identified PTMs

31% (55/177) of our cross-linked peptides contained a PTM such as acetylation, methylation or phosphorylation (see Table S1). A search for these PTMs using GPMDB (https://gpmdb.thegpm.org/) revealed that 95% of these PTMs had not been previously observed. After considering the possibility that these PTMs might be biologically important, we selected 3 different PTM-modified cross-links for further study from proteins in diverse cellular pathways; Pim1 (mitochondrial proteostasis), Mtw1 (chromosome segregation) and Ste11 (pheromone and osmotic stress response).

HIR complex is novel client of Hsp70

The histone regulator (HIR) protein complex regulates histone gene transcription, nucleosome formation and heterochromatic gene silencing (Mazzoni et al., 2005; Sharp et al., 2005). Our XL-MS analysis revealed a novel direct interaction between Ssa1 and HIR complex components Hir1 and Hir2. We observed cross-linking between the SBD of Ssa1 and residues K435 of Hir1 and K452 of Hir2, adjacent to their respective nuclear localization signals (Figure 4A and 4B). To validate our XL-MS finding, we carried out Co-IP and immunoblotting of Hir1 and Hir2 with key chaperone components Ssa1, Sse1, Hsp82 and Ydj1. These experiments confirmed a strong association between HIR and the chaperones tested (Figure 4C). Furthermore, we confirmed that Hir1 and Hir2 are

bona fide Ssa1 client proteins by demonstrating that loss of Ssa1 function resulted in Hir1 and Hir2 destabilization (Figure 4D).

To demonstrate evolutionary conservation of the identified chaperone-HIR interaction, we examined interaction between human Hsc70 and HIRA, the major HIR complex protein in human cells. Consistent with our results in yeast, HA-HIRA co-immunoprecipitated with Hsc70, Hsp110, Hsp90, DNAJA1 (Figure 4E). To examine dependence of HIRA on Hsc70 chaperone activity, we treated HEK293 cells with the Hsp70 inhibitor JG-98 and monitored HIRA abundance over time. HIRA levels rapidly decreased after JG-98 addition, with HIRA becoming undetectable after 2 hours (Figure 4F). Given that in our system HA-HIRA was expressed under the constitutive human cytomegalovirus (CMV) promoter, we hypothesized that the effect we observed on HIRA abundance could be explained by protein degradation. Supporting this hypothesis, addition of the proteasomal inhibitor bortezomib prevented JG-98 dependent HIRA loss (Figure 4F).

Taken together, our results suggest that HIR complex proteins are client proteins of the Hsp70 chaperone system in yeast and mammalian cells.

Hsp70 plays a dual role in mitochondrial Pim1 protease activity

Pim1 is an ATP-dependent yeast Lon protease that is involved in degradation of misfolded mitochondrial proteins, required for mitochondrial maintenance and biogenesis (Van Dyck et al., 1994). Our XL-MS data revealed an interaction between the Pim1 protease domain and the N-terminal domain of Ssa1 (Figure 5A, 5B). We first validated the Pim1 interaction with Ssa1 and associated co-chaperones using co-

immunoprecipitation and immunoblotting (Figure 5C). The clearance of mitochondrial aggregates is important for cell homeostasis and, as such, many organisms express a Pim1 homologue. To examine whether the Ssa1-Pim1 interaction is conserved in mammalian cells, we performed an equivalent experiment to that shown in 5C, using mammalian Lonp-1 as the bait. Similar to our observations in yeast, mammalian Lonp-1 interacted with chaperone proteins including Hsc70, Hsp110, Hsp90 and DNAJA1 (Figure 5D). In order to determine if Lonp-1 is a client protein of Hsp70, we treated HEK293 cells with Hsp70 inhibitor JG-98 and observed Lonp-1 degradation after 2 hours of treatment. Treatment of HEK293 cells with bortezomib before addition of JG-98 prevented loss of Lonp-1, confirming that Lonp-1 is a client protein of Hsc70 (Figure 5E).

The Pim1 portion of the Ssa1-Pim1 cross-linked peptide contained a previously undiscovered Pim1 phosphorylation site (S974). Given its proximity to the interaction surface between Ssa1 and Pim1, we hypothesized that this phosphorylation site might be important for Pim1 function. To examine the impact of S974 phosphorylation on Pim1 function, we expressed Pim1 mutants lacking this phosphorylation site (S974A) or mimicking constitutive phosphorylation (S974D) from the regulatable *CUP1* promoter in cells lacking Pim1. Although S974A cells grew at a similar rate to WT in standard growth media, S974D cells were substantially inhibited for growth (Figure 5F). To determine whether the growth defect of the S974D mutant was due to irregular mitochondrial protein aggregation, we examined the aggregation behavior of a previously established mitoFluc reporter (Ruan et al., 2020; Ruan et al., 2017). S974D mutants were unable to clear mitochondrial protein aggregates (Figure 5F, Figure 5G). To query whether loss of Pim1 function in the S974D mutant was due to its mislocalization, we examined localization of

GFP-tagged WT, S974A and S974D Pim1 proteins. Intriguingly, Pim1 localization was unaffected by the phosphorylation state of S974 (Figure S2A).

Like many proteases, Pim1 undergoes self-cleavage to achieve full maturation and protease activity (Ondrovicova et al., 2005). We examined Pim1 processing in WT, S974A and S974D cells. In contrast to both WT and S974A, S974D resolved as a single band on SDS-PAGE, suggesting that Pim1 self-cleavage and maturation was compromised in S974D cells (Figure 5H, S2C). The proximity of S974 to the identified Ssa1-Pim1 cross-linked peptides suggested that this residue was important to the Ssa1-Pim1 interaction. Immunoprecipitation of Pim1 variants demonstrated that, although not critical for Ssa1-Pim1 interaction, S974 phosphorylation significantly enhanced the interaction between the two proteins (Figure 5I).

Based on our results shown in Figures 5A-5I, we hypothesized that Ssa1 may bind to phosphorylated Pim1 to inhibit its function. To examine Pim1 activity in the absence of endogenous Ssa1 activity, we expressed recombinant yeast Pim1 (WT, S974A and S974D) in *E. coli* (Figure 5J). In contrast to our findings in 5H, Pim1 self-cleavage was independent of S974 phosphorylation status in the absence of Ssa1 (Figure 5J). Upon co-expression of Pim1 and Ssa1 in bacteria, self-cleavage of Pim1 was restored only in the S974D mutant (Figure 5J). Taken together, our findings demonstrate that fascinatingly, Pim1 is not only a novel client of Ssa1, but that Ssa1 can prevent phosphorylation-mediated Pim1 self-cleavage (Figure 5K).

Ssa1 regulates kinetochore function via Mtw1

Mtw1 is an essential component of the MIND kinetochore complex and it connects kinetochore subunits binding DNA to those associated with microtubules, rendering it

critical to kinetochore assembly. Direct interaction between the NBD of Ssa1 and the head domain of Mtw1 was observed by XL-MS (Figure 6A, 6B). To confirm direct interaction between Mtw1 and the Hsp70 chaperone system proteins (Ssa1, Sse1, Hsp82 and Ydj1) we used a Co-IP and immunoblotting approach, similar to the one used above for other identified direct interactors (Figure 6C). Perturbation of Ssa1 function destabilized Mtw1 confirming its status as a new Hsp70 client protein in yeast (Figure 6D).

The mammalian equivalent of Mtw1, Mis12, is critical for correct kinetochore attachment (Petrovic et al., 2010). The Ssa1-Mtw1 interaction is conserved in mammalian cells as evidenced by the successful co-purification of Mis12 with Hsc70, Hsp110, Hsp90 and DNAJA1 (Figure 6E). Furthermore, treatment of HEK293 cells with Hsp70 inhibitor JG-98 resulted in loss of Mis12, and addition of the proteasomal inhibitor bortezomib prevented JG-98-mediated Mis12 destruction, showing that inhibition of Hsp70 leads to proteasomal degradation of Mis12 (Figure 6F). Taken together, our results suggest that Mis12 is a novel client protein of Hsp70.

The identified site of interaction between Mtw1 and Ssa1 contained a previously undiscovered phosphorylation site, Y86 on Mtw1 (Figure 6A). Previous studies have shown that Y86 is at the interface between Mtw1 and a second essential kinetochore subunit, Mif2 (Dimitrova et al., 2016; Hornung et al., 2011; Killinger et al., 2020). Haploid yeast cells expressing the non-phosphorylatable Y86F Mtw1 mutant protein were viable but compromised for growth on the microtubule-perturbing agent benomyl (Figure 6G, S3A and B). Notably, we were not able to generate cells expressing a phospho-mimetic Y86E Mtw1 mutant protein. We compared Mtw1 localization at the kinetochore in both WT and Y86F mutant strains. Y86F cells showed a significantly increased accumulation

of Mtw1 at the kinetochore compared to wild-type cells (Figure 6H and 6I). Although the Y86F mutation significantly impacted interaction between Mtw1 and either Hsp82 or Ydj1, Ssa1 was unaffected by the Y86F mutation (Figure 6J). Taken together our data suggests phosphorylation of Mtw1 and its interaction with Ssa1 affects its incorporation into kinetochores (Figure 6K).

Ssa1 is involved in the selective activation of Ste11-mediated signaling

Ste11 is a MEK kinase involved in the cellular responses to both pheromone and hypo-osmolarity (Harris et al., 2001; Nishimura et al., 2016; Tatebayashi et al., 2006; Tatebayashi et al., 2020) (Figure 7A). It was an encouraging validation of our XL-MS methodology to observe direct interaction between the N-terminus of Ssa1 and the unstructured regulatory domain of Ste11, one of the first identified client proteins of Hsp90 (Figure 7B). As with Mtw1 and Pim1, the Ssa1-Ste11 peptide contained a previous undiscovered PTM, dimethylation on Ste11 R305. To determine the functional importance of dimethylation of Ste11 R305, we created the non-methylatable mutant R305A and dimethylation-mimic R305F and expressed these in cells lacking Ste11. To examine the impact of R305 on the pheromone response, we assessed the ability of Ste11 R305A and R305F to form halos in response to alpha factor, activate a FUS1-LacZ reporter and promote Fus3 phosphorylation. In all 3 experiments, both R305A and R305F behaved in a similar manner to WT (Figures 7C, D, E).

Although the R305 dimethylation status had minimal impact on the pheromone response, previous studies have demonstrated that some hyper-active mutations within this region (e.g. *STE11-Q301P* or *STE11-DDD*) rescue the osmo-adaptation defect caused by deletion of upstream Ste20 kinase upon high osmolarity (Tatebayashi et al.,

2006; Tatebayashi et al., 2020). We examined the ability of Ste11 R305 mutants to complement the loss of Ste11 in response to osmotic shock. Because Ste11 is essential for Hog1 MAPK activation by osmostress only when the other upstream pathway (the SLN1 branch) is inactivated, we deleted the *SSK2* and *SSK22* genes encoding the MEKKs for the SLN1 branch from the host cells (Figure 7A). As with the pheromone response, the R305 dimethylation status appeared to be dispensable for Ste11 function in this regard (Figure 7F, upper panel). It is known that deletion of the upstream components of the Ste11-osmotic response pathway such as Ste20, renders cells sensitive to media containing NaCl (Nishimura et al., 2016; Tatebayashi et al., 2006; Tatebayashi et al., 2020). Interestingly, we found that while expression of WT and R305A Ste11 in cells lacking native Ste11, Ssk2, Ssk22 and Ste20 had no discernible effect on osmotic resistance, R305F Ste11 rendered cells resistant to NaCl (Figure 7F, lower panel). To determine the impact of these R305 mutations on Hog1 activation, we performed reporter assays using the Hog1 reporter *8xCRE-lacZ* on cells examined in 7F. The R305F mutant was able to induce *CRE*-mediated transcription at a level several fold greater than WT Ste11, albeit at a lower level than that observed for previously characterized hyperactive Ste11 mutants DDD and Q301P (Figure 7G). To determine whether this R305F phenotype in was specific to the osmotic stress response in ste11/ssk2/ssk22/ste20Δ cells, we performed a halo assay on the cells from 7G. In contrast to the results in 7F and 7G, Ste11 R305F was indistinguishable from WT or R305A (Figure 7H).

We wondered whether R305 dimethylation might impact interaction with either Ssa1 or Ydj1, particularly given that the Ssa1-Ste11 cross-link was formed adjacent to

the R305 site. Interaction studies using immunoprecipitated Ste11 suggest that R305 dimethylation was not essential for interaction with Ssa1 or Ydj1 (Figure 7I). Taken together, our data indicates a novel interaction of Ssa1 with the unstructured regulatory domain of Ste11 adjacent to a dimethylation site that impacts only osmotic signaling (Figure 7J).

Discussion

Towards a comprehensive Hsp70 interactome

The identification and characterization of new chaperone interactions is important to understand the fundamental process of protein folding (Bohen et al., 1995). This knowledge can ultimately lead to the design of novel therapies that rely on the manipulation of chaperone function. While large-scale interactome studies of chaperones have been attempted previously, the methods used in these attempts have associated drawbacks that prevent a comprehensive analysis of the system (Koegl and Uetz, 2007; Yugandhar et al., 2019). For example, several of these technologies such as LUMIER are performed on purified proteins and thus might not have the dynamic range to detect the impacts of PTMs and scaffold proteins (Taipale, 2018; Taipale et al., 2014). Other cell-based assays such as AP-MS, Y2H and proximity labelling lack the ability to distinguish direct from bridged interactions. All of these drawbacks can be addressed by using the XL-MS technology we describe in this report.

XL-MS methodologies provide the ability to both stabilize transient interactions and allow characterization of the interaction surface between two proteins (Leitner et al., 2016; Liu et al., 2015). Recently, this innovative technology was used to obtain a more complete

interactor list for Hsp90, providing a more accurate picture of its molecular dynamics (Chavez et al., 2016). For these reasons, we have used XL-MS to characterize the Hsp70 interactome in yeast. Our study identified a total of 1510 different proteins complexed with Hsp70, 238 of which were confirmed to be direct interactors. Importantly, 121 of these direct interactions had never been previously observed, validating the use of XL-MS technology to comprehensively study the Hsp70 interactome in the future. It is interesting to speculate what the remaining 1274 interactors represent. They may be bridged interactors present in association with Hsp70 complexes. If that is the case, it would suggest that large-scale datasets claiming to identify direct chaperone interactions might need to be revisited for accuracy. On the other hand, these interactions may be direct *bona fide* interactors that for technical reasons were unable to be cross-linked to Ssa1.

Previous *in vitro* studies suggested that the majority of interactions would be localized to the CTD of Hsp70, the domain recognized as being responsible for binding and processing of Hsp70 client proteins (Radons, 2016). Using our XL-MS method, we identified new Ssa1-interactions that map to other Hsp70 domains (Fig. 3A). Unexpectedly, 79% of the total interactions identified mapped to the NBD of Hsp70 (Fig. S1 B and C). Even after accounting for the number of cross-linkable lysines present on each Hsp70 domain, the NBD had over sixfold the number of interactions compared to the CTD. Biologically, there may be several explanations for this result. Firstly, it is possible that during the client protein-binding process, there are multiple interactions between chaperone and client-protein that engage the entirety of Hsp70. Although this phenomenon has been observed *in vitro* between recombinant Hsp70 and single client proteins, our work is the first to make a similar observation at the interactome level

(Mashaghi et al., 2016). Secondly, we may be detecting the interaction of Hsp70 in fully-formed protein complexes. Finally, several of the N-terminal interactions may represent novel co-chaperones/regulators of Hsp70.

Our goal was to identify a comprehensive clientome of Hsp70. To achieve this, we did not replenish ATP during the cross-linking and purification process, skewing the complexes towards co-chaperone free, client-bound Hsp70 complexes. In agreement with this, although several co-chaperones (Sse1, Cct8, Ydj1) were detected in complexes with Hsp70, very few were identified in our cross-linked samples. Although beyond the scope of this study, future experiments may entail purification of Hsp70 complexes in different stages of the folding cycle to trap co-chaperones rather than clients.

While proteomics methods can undoubtedly produce non-native interactions, all the hits selected for follow up in this report were confirmed to be genuine Hsp70 interactors in both yeast and mammalian cells. Given the stress-dependent nature of the Hsp70 interactome, it will be important to perform variations of this XL-MS experiment under different stress conditions such as heat, cell cycle stage, DNA damage response and nutrient deprivation.

Understanding novel Ssa1-Ssa1 interactions

An advantage of XL-MS methodologies is the ability to detect a wider range of information about protein folding and structure. For example, in the case of Hsp90, XL-MS has been used to understand protomer conformational changes upon ATP binding (Chavez et al., 2016). In this study, we identified 177 internal Ssa1-Ssa1 cross-links. Although the structure of full length Ssa1 protein has yet to be obtained, sequence similarity to bacterial

and mammalian Hsp70 strongly suggests that Ssa1 forms similar ATP and ADP-bound conformations (Bertelsen et al., 2009; Rosenzweig et al., 2019b; Zhu et al., 1996). Serving as an internal control to our experiment, the majority of obtained Ssa1-Ssa1 peptides could be matched to these structures. We were surprised by the number of remaining peptides that could not be matched to any known monomeric Hsp70 structure. Deeper analysis of these peptides revealed that these were likely the result of cross-linking of *two different* Ssa1 molecules. The evidence supporting this is twofold. Firstly, the distance between these cross-linked Ssa1-Ssa1 peptides exceeded the known DSSO cross-linker length. Secondly, several of the cross-linked Ssa1-Ssa1 peptides were symmetrical; the peptides on each side of the cross-link were the same. While clearly not at the same stoichiometry as Hsp90, several studies on bacterial and human Hsp70 have demonstrated a capacity for the purified chaperone to form higher-order structures (Bertelsen et al., 2009; Liu et al., 2017; Morgner et al., 2015; Sarbeng et al., 2015; Takakuwa et al., 2019; Trcka et al., 2019) Expression of a dimerization-deficient DnaK in bacteria produces viable cells that are sensitive to thermal stress, suggesting that dimerization is needed for a subset of DnaK functions (Liu et al., 2017). Through both co-immunoprecipitation and BiFC, we demonstrate for the first time that yeast Ssa1 can also form dimers in cells. These dimers are almost exclusively localized to the nucleus, suggesting an nuclear-specific function. While the role of the Ssa1 dimer remains to be explored, given that regulation of the heat shock response by HSF occurs in the nucleus, we hypothesize that dimerization may be a novel way to regulate HSF activation in cells.

Using sites of Hsp70 interaction to reveal novel PTMs of functional relevance on client proteins

Interactions with molecular chaperones are critical for supporting the function of proteins involved in signal transduction, particularly those involved in PTMs such as kinases or acetylases (Chen et al., 2014; O'Regan et al., 2015; Tao et al., 2016). Some of these interactions are quite stable, with client proteins requiring continuous chaperone interaction for activity (Kim et al., 2013). Others are transient, where full client protein maturation and activity requires rapid chaperone dissociation (Rosenzweig et al., 2019b). However, there is also a growing body of work that shows that PTMs play an important and novel role in chaperone interactions. For example, the client-phosphorylation status of the Hsp90-Mpk1 and Hsp90-ERK5 complexes have been shown to be important for their function (Piper et al., 2006). The chaperone code can also regulate interactions with many chaperones/co-chaperones including Hsp90, Hsp70, HSF, Cdc37 (Cloutier and Coulombe, 2013; Nitika et al., 2020; Nitika and Truman, 2017). While these PTMs have been identified on a one-at-a-time basis, ours is the first study to identify important chaperone-PTM interactions on a much larger scale.

In this work, we have followed up on three Hsp70 clients that contain novel PTMs on the site of interaction with Ssa1- Mtw1, Pim1 and Ste11. In each of these cases, while the client protein PTMs had been previously undiscovered, we have shown them to regulate novel and distinct (and very different) client protein functionalities. For Mtw1, PTM appears to regulate its localization, required for full functionality. For Pim1, S974 phosphorylation doesn’t impact stability or localization, but rather self-processing and proteolytic activity. For Ste11, one the canonical Hsp90 clients, our working model is that

dimethylation regulates the transition between inactive and active Ste11 conformations, either independent of or in conjunction with its regulation by phosphorylation. While beyond the scope of this study, we hypothesize that this dimethylation is selectively impacting interactions of Ste11 with components of the osmotic stress response pathway such as Ste50.

Future studies will aim to decipher the stresses and enzymes that regulate these PTMs in addition to teasing apart their hierarchy of interaction with Ssa1. We currently have two working models; in the first the presence of the PTM recruits Hsp70 to alter client protein interactions and therefore function. In the second, Ssa1 is acting as a "protective cover" over the novel PTM, trapping the PTM in its on/off state, ultimately altering the kinetics of client activation. These two models, while reasonable, are hard to test given that Ssa1 is essential for cell growth and acts at multiple points in the signal transduction pathways involved.

This study has unveiled new regulatory mechanisms for Hsp70 and its client proteins. In doing so, we have established novel tools, methods, and workflows that will allow the field to achieve a more complete understanding of chaperones and the ways in which cells use them to integrate signal transduction pathways.

Acknowledgements

This work was supported by the NIH (R15GM139059 and R01GM139885 to AWT, R01GM057769 to PMP), the Queen Mary University of London and the Francis Crick Institute (Cancer Research UK—FC001183; UK Medical Research Council—FC001183

and the Wellcome Trust—FC001183 to PHT), a grant from Re-Stem Biotech to R.L., the JSPS Grants-in-Aid for Scientific Research (KAKENHI) (21H02422 to KT), the Institute for Fermentation, Osaka (G-2021-2-082 to KT). We thank Dr. Paola Lopez-Duarte for the use of her confocal microscope.

Author Contributions

N, BZ, JET, MJW and KT conducted experiments and analyzed data with assistance from AWT and PMP. JTK, JK, RH and LF assisted with XL-MS experiments and data analysis. LR, YW and RL, contributed to the Pim1 mutation and microscopy analysis. MTT, CK and PT performed the Mtw1 microscopy. N and AWT designed the study, interpreted the data, and wrote the first draft of the manuscript. VAS edited and revised the manuscript. AWT supervised the project. All authors reviewed and approved the final manuscript.

References

Artigues, A., Iriarte, A., and Martinez-Carrion, M. (2002). Binding to chaperones allows import of a purified mitochondrial precursor into mitochondria. J Biol Chem *277*, 25047-25055.

Beltrao, P., Albanese, V., Kenner, L.R., Swaney, D.L., Burlingame, A., Villen, J., Lim, W.A., Fraser, J.S., Frydman, J., and Krogan, N.J. (2012). Systematic functional prioritization of protein posttranslational modifications. Cell *150*, 413-425.

Bertelsen, E.B., Chang, L., Gestwicki, J.E., and Zuiderweg, E.R. (2009). Solution conformation of wild-type E. coli Hsp70 (DnaK) chaperone complexed with ADP and substrate. Proc Natl Acad Sci U S A *106*, 8471-8476.

Bohen, S.P., Kralli, A., and Yamamoto, K.R. (1995). Hold 'em and fold 'em: chaperones and signal transduction. Science *268*, 1303-1304.

Bush, G.L., and Meyer, D.I. (1996). The refolding activity of the yeast heat shock proteins Ssa1 and Ssa2 defines their role in protein translocation. J Cell Biol *135*, 1229-1237.

Catherman, A.D., Skinner, O.S., and Kelleher, N.L. (2014). Top Down proteomics: facts and perspectives. Biochem Biophys Res Commun *445*, 683-693.

Chavez, J.D., Schweppe, D.K., Eng, J.K., and Bruce, J.E. (2016). In Vivo Conformational Dynamics of Hsp90 and Its Interactors. Cell Chem Biol *23*, 716-726.

Chen, Y.J., Lai, K.C., Kuo, H.H., Chow, L.P., Yih, L.H., and Lee, T.C. (2014). HSP70 colocalizes with PLK1 at the centrosome and disturbs spindle dynamics in cells arrested in mitosis by arsenic trioxide. Arch Toxicol *88*, 1711-1723.

Chirico, W.J., Markey, M.L., and Fink, A.L. (1998). Conformational changes of an Hsp70 molecular chaperone induced by nucleotides, polypeptides, and N-ethylmaleimide. Biochemistry *37*, 13862-13870.

Cloutier, P., and Coulombe, B. (2013). Regulation of molecular chaperones through post-translational modifications: decrypting the chaperone code. Biochim Biophys Acta *1829*, 443-454.

Dimitrova, Y.N., Jenni, S., Valverde, R., Khin, Y., and Harrison, S.C. (2016). Structure of the MIND Complex Defines a Regulatory Focus for Yeast Kinetochore Assembly. Cell *167*, 1014-1027 e1012.

Dubrez, L., Causse, S., Borges Bonan, N., Dumetier, B., and Garrido, C. (2019). Heat-shock proteins: chaperoning DNA repair. Oncogene.

Dushukyan, N., Dunn, D.M., Sager, R.A., Woodford, M.R., Loiselle, D.R., Daneshvar, M., Baker-Williams, A.J., Chisholm, J.D., Truman, A.W., Vaughan, C.K.*, et al.* (2017). Phosphorylation and Ubiquitination Regulate Protein Phosphatase 5 Activity and Its Prosurvival Role in Kidney Cancer. Cell Rep *21*, 1883-1895.

Frydman, J., Nimmesgern, E., Ohtsuka, K., and Hartl, F.U. (1994). Folding of nascent polypeptide chains in a high molecular mass assembly with molecular chaperones. Nature *370*, 111-117.

Gentzel, M., Pardo, M., Subramaniam, S., Stewart, A.F., and Choudhary, J.S. (2019). Proteomic navigation using proximity-labeling. Methods *164-165*, 67-72.

Gupta, A., Puri, A., Singh, P., Sonam, S., Pandey, R., and Sharma, D. (2018). The yeast stress inducible Ssa Hsp70 reduces alpha-synuclein toxicity by promoting its degradation through autophagy. PLoS Genet *14*, e1007751.
Harris, K., Lamson, R.E., Nelson, B., Hughes, T.R., Marton, M.J., Roberts, C.J., Boone, C., and Pryciak, P.M. (2001). Role of scaffolds in MAP kinase pathway specificity revealed by custom design of pathway-dedicated signaling proteins. Curr Biol *11*, 1815-1824.
Hartl, F.U., Bracher, A., and Hayer-Hartl, M. (2011). Molecular chaperones in protein folding and proteostasis. Nature *475*, 324-332.
Hornung, P., Maier, M., Alushin, G.M., Lander, G.C., Nogales, E., and Westermann, S. (2011). Molecular architecture and connectivity of the budding yeast Mtw1 kinetochore complex. J Mol Biol *405*, 548-559.
Killinger, K., Bohm, M., Steinbach, P., Hagemann, G., Bluggel, M., Janen, K., Hohoff, S., Bayer, P., Herzog, F., and Westermann, S. (2020). Auto-inhibition of Mif2/CENP-C ensures centromere-dependent kinetochore assembly in budding yeast. EMBO J *39*, e102938.
Kim, Y.E., Hipp, M.S., Bracher, A., Hayer-Hartl, M., and Hartl, F.U. (2013). Molecular chaperone functions in protein folding and proteostasis. Annual review of biochemistry *82*, 323-355.
Koegl, M., and Uetz, P. (2007). Improving yeast two-hybrid screening systems. Brief Funct Genomic Proteomic *6*, 302-312.
Ledesma-Fernandez, E., and Thorpe, P.H. (2015). Fluorescent foci quantitation for high-throughput analysis. J Biol Methods *2*.
Leitner, A., Faini, M., Stengel, F., and Aebersold, R. (2016). Crosslinking and Mass Spectrometry: An Integrated Technology to Understand the Structure and Function of Molecular Machines. Trends Biochem Sci *41*, 20-32.
Liu, F., Rijkers, D.T., Post, H., and Heck, A.J. (2015). Proteome-wide profiling of protein assemblies by cross-linking mass spectrometry. Nat Methods *12*, 1179-1184.
Liu, Q., Li, H., Yang, Y., Tian, X., Su, J., Zhou, L., and Liu, Q. (2017). A disulfide-bonded DnaK dimer is maintained in an ATP-bound state. Cell Stress Chaperones *22*, 201-212.
Mashaghi, A., Bezrukavnikov, S., Minde, D.P., Wentink, A.S., Kityk, R., Zachmann-Brand, B., Mayer, M.P., Kramer, G., Bukau, B., and Tans, S.J. (2016). Alternative modes of client binding enable functional plasticity of Hsp70. Nature *539*, 448-451.
Mazzoni, C., Palermo, V., Torella, M., and Falcone, C. (2005). HIR1, the co-repressor of histone gene transcription of Saccharomyces cerevisiae, acts as a multicopy suppressor of the apoptotic phenotypes of the LSM4 mRNA degradation mutant. FEMS Yeast Res *5*, 1229-1235.
Millson, S.H., Truman, A.W., King, V., Prodromou, C., Pearl, L.H., and Piper, P.W. (2005). A two-hybrid screen of the yeast proteome for Hsp90 interactors uncovers a novel Hsp90 chaperone requirement in the activity of a stress-activated mitogen-activated protein kinase, Slt2p (Mpk1p). Eukaryot Cell *4*, 849-860.
Morgner, N., Schmidt, C., Beilsten-Edmands, V., Ebong, I.O., Patel, N.A., Clerico, E.M., Kirschke, E., Daturpalli, S., Jackson, S.E., Agard, D.*, et al.* (2015). Hsp70 forms antiparallel dimers stabilized by post-translational modifications to position clients for transfer to Hsp90. Cell Rep *11*, 759-769.

Nishimura, A., Yamamoto, K., Oyama, M., Kozuka-Hata, H., Saito, H., and Tatebayashi, K. (2016). Scaffold Protein Ahk1, Which Associates with Hkr1, Sho1, Ste11, and Pbs2, Inhibits Cross Talk Signaling from the Hkr1 Osmosensor to the Kss1 Mitogen-Activated Protein Kinase. Mol Cell Biol *36*, 1109-1123.
Nitika, Porter, C.M., Truman, A.W., and Truttmann, M.C. (2020). Post-translational modifications of Hsp70 family proteins: Expanding the chaperone code. J Biol Chem *295*, 10689-10708.
Nitika, and Truman, A.W. (2017). Cracking the Chaperone Code: Cellular Roles for Hsp70 Phosphorylation. Trends Biochem Sci *42*, 932-935.
O'Regan, L., Sampson, J., Richards, M.W., Knebel, A., Roth, D., Hood, F.E., Straube, A., Royle, S.J., Bayliss, R., and Fry, A.M. (2015). Hsp72 is targeted to the mitotic spindle by Nek6 to promote K-fiber assembly and mitotic progression. J Cell Biol *209*, 349-358.
Ondrovicova, G., Liu, T., Singh, K., Tian, B., Li, H., Gakh, O., Perecko, D., Janata, J., Granot, Z., Orly, J.*, et al.* (2005). Cleavage site selection within a folded substrate by the ATP-dependent lon protease. J Biol Chem *280*, 25103-25110.
Petrovic, A., Pasqualato, S., Dube, P., Krenn, V., Santaguida, S., Cittaro, D., Monzani, S., Massimiliano, L., Keller, J., Tarricone, A.*, et al.* (2010). The MIS12 complex is a protein interaction hub for outer kinetochore assembly. J Cell Biol *190*, 835-852.
Piper, P.W., Truman, A.W., Millson, S.H., and Nuttall, J. (2006). Hsp90 chaperone control over transcriptional regulation by the yeast Slt2(Mpk1)p and human ERK5 mitogen-activated protein kinases (MAPKs). Biochem Soc Trans *34*, 783-785.
Radons, J. (2016). The human HSP70 family of chaperones: where do we stand? Cell Stress Chaperones *21*, 379-404.
Rosenzweig, R., Nillegoda, N.B., Mayer, M.P., and Bukau, B. (2019a). The Hsp70 chaperone network. Nat Rev Mol Cell Biol.
Rosenzweig, R., Nillegoda, N.B., Mayer, M.P., and Bukau, B. (2019b). The Hsp70 chaperone network. Nat Rev Mol Cell Biol *20*, 665-680.
Ruan, L., McNamara, J.T., Zhang, X., Chang, A.C., Zhu, J., Dong, Y., Sun, G., Peterson, A., Na, C.H., and Li, R. (2020). Solid-phase inclusion as a mechanism for regulating unfolded proteins in the mitochondrial matrix. Sci Adv *6*, eabc7288.
Ruan, L., Zhou, C., Jin, E., Kucharavy, A., Zhang, Y., Wen, Z., Florens, L., and Li, R. (2017). Cytosolic proteostasis through importing of misfolded proteins into mitochondria. Nature *543*, 443-446.
Sarbeng, E.B., Liu, Q., Tian, X., Yang, J., Li, H., Wong, J.L., Zhou, L., and Liu, Q. (2015). A functional DnaK dimer is essential for the efficient interaction with Hsp40 heat shock protein. J Biol Chem *290*, 8849-8862.
Sharp, J.A., Rizki, G., and Kaufman, P.D. (2005). Regulation of histone deposition proteins Asf1/Hir1 by multiple DNA damage checkpoint kinases in Saccharomyces cerevisiae. Genetics *171*, 885-899.
Swaney, D.L., Beltrao, P., Starita, L., Guo, A., Rush, J., Fields, S., Krogan, N.J., and Villen, J. (2013). Global analysis of phosphorylation and ubiquitylation cross-talk in protein degradation. Nature methods *10*, 676-682.
Taipale, M. (2018). Quantitative Profiling of Chaperone/Client Interactions with LUMIER Assay. Methods Mol Biol *1709*, 47-58.

Taipale, M., Tucker, G., Peng, J., Krykbaeva, I., Lin, Z.Y., Larsen, B., Choi, H., Berger, B., Gingras, A.C., and Lindquist, S. (2014). A quantitative chaperone interaction network reveals the architecture of cellular protein homeostasis pathways. Cell *158*, 434-448.
Takakuwa, J.E., Nitika, Knighton, L.E., and Truman, A.W. (2019). Oligomerization of Hsp70: Current Perspectives on Regulation and Function. Front Mol Biosci *6*, 81.
Tao, Y., Messer, J.S., Goss, K.H., Hart, J., Bissonnette, M., and Chang, E.B. (2016). Hsp70 exerts oncogenic activity in the Apc mutant Min mouse model. Carcinogenesis *37*, 731-739.
Tatebayashi, K., Yamamoto, K., Tanaka, K., Tomida, T., Maruoka, T., Kasukawa, E., and Saito, H. (2006). Adaptor functions of Cdc42, Ste50, and Sho1 in the yeast osmoregulatory HOG MAPK pathway. EMBO J *25*, 3033-3044.
Tatebayashi, K., Yamamoto, K., Tomida, T., Nishimura, A., Takayama, T., Oyama, M., Kozuka-Hata, H., Adachi-Akahane, S., Tokunaga, Y., and Saito, H. (2020). Osmostress enhances activating phosphorylation of Hog1 MAP kinase by mono-phosphorylated Pbs2 MAP2K. EMBO J *39*, e103444.
Trcka, F., Durech, M., Vankova, P., Chmelik, J., Martinkova, V., Hausner, J., Kadek, A., Marcoux, J., Klumpler, T., Vojtesek, B*., et al.* (2019). Human Stress-inducible Hsp70 Has a High Propensity to Form ATP-dependent Antiparallel Dimers That Are Differentially Regulated by Cochaperone Binding. Molecular & cellular proteomics : MCP *18*, 320-337.
Truman, A.W., Kristjansdottir, K., Wolfgeher, D., Hasin, N., Polier, S., Zhang, H., Perrett, S., Prodromou, C., Jones, G.W., and Kron, S.J. (2012). CDK-dependent Hsp70 Phosphorylation controls G1 cyclin abundance and cell-cycle progression. Cell *151*, 1308-1318.
Truman, A.W., Kristjansdottir, K., Wolfgeher, D., Ricco, N., Mayampurath, A., Volchenboum, S.L., Clotet, J., and Kron, S.J. (2015). Quantitative proteomics of the yeast Hsp70/Hsp90 interactomes during DNA damage reveal chaperone-dependent regulation of ribonucleotide reductase. Journal of proteomics *112*, 285-300.
Van Dyck, L., Pearce, D.A., and Sherman, F. (1994). PIM1 encodes a mitochondrial ATP-dependent protease that is required for mitochondrial function in the yeast Saccharomyces cerevisiae. J Biol Chem *269*, 238-242.
Vidal, M., Brachmann, R.K., Fattaey, A., Harlow, E., and Boeke, J.D. (1996). Reverse two-hybrid and one-hybrid systems to detect dissociation of protein-protein and DNA-protein interactions. Proc Natl Acad Sci U S A *93*, 10315-10320.
Yang, Y., Fiskus, W., Yong, B., Atadja, P., Takahashi, Y., Pandita, T.K., Wang, H.G., and Bhalla, K.N. (2013). Acetylated hsp70 and KAP1-mediated Vps34 SUMOylation is required for autophagosome creation in autophagy. Proc Natl Acad Sci U S A *110*, 6841-6846.
Yugandhar, K., Gupta, S., and Yu, H. (2019). Inferring Protein-Protein Interaction Networks From Mass Spectrometry-Based Proteomic Approaches: A Mini-Review. Comput Struct Biotechnol J *17*, 805-811.
Zhao, R., Davey, M., Hsu, Y.C., Kaplanek, P., Tong, A., Parsons, A.B., Krogan, N., Cagney, G., Mai, D., Greenblatt, J*., et al.* (2005). Navigating the chaperone network: an integrative map of physical and genetic interactions mediated by the hsp90 chaperone. Cell *120*, 715-727.

Zhu, X., Zhao, X., Burkholder, W.F., Gragerov, A., Ogata, C.M., Gottesman, M.E., and Hendrickson, W.A. (1996). Structural analysis of substrate binding by the molecular chaperone DnaK. Science *272*, 1606-1614.

Figure Legends

Figure 1. Cross-linking mass spectrometry of Ssa1 complexes. (A) Experimental workflow of cross-linking mass spectrometry of Ssa1 complexes purified from yeast cells. (B) Venn diagram representing Ssa1 complexes found in conventional IP and DSSO treated IP. (C) Pie chart showing types of cross links identified from XL-MS analysis. (D) Gene ontology analysis of DSSO treated Ssa1 immunoprecipitated complexes and crosslinked Ssa1 complexes using TheCellMap.org.

Figure 2. A proportion of Ssa1 exists as dimer. (A) Ssa1 cross links identified from XL-MS analysis mapped on the monomeric structure of Ssa1 in open and closed conformation. (B) Ssa1 cross links mapped on the domains of Ssa1 in open and closed conformation. (C) Internal and External Ssa1 cross links were mapped on the dimeric structure of Ssa1 (4JNE). (D) Internal and External cross links were mapped on the crystal structure of Ssa1 (4JNE). (E) Immunoblot analysis of Flag-tagged Ssa1 purified from cells expressing HA-tagged Ssa1. (F) Fluorescence images of diploid cells expressing the N-terminally VN- and VC- tagged Ssa1. DAPI was used as a nuclear marker. Scale bars are10 μM. (G) Western blot analysis of Flag-tagged Ssa1 and Flag-tagged Ssa1-V435F mutants purified from cells expressing HA-tagged Ssa1.

Figure 3. Novel clients and post translationally modified clients identified on yeast Hsp70 based on XL-MS. (A) Schematic representation of 177 inter-protein crosslinks

and identified post-translational modifications on domains of Hsp70. (B) Functional classification of direct Hsp70-client peptides. (C) Western blot analysis of HA-tag immunoprecipitated Cct8, Pcl7, Ura8 and Sse1 from yeast cells.

Figure 4. HIR complex is a novel client of Hsp70 in yeast and humans. (A) Schematic representation of Ssa1-Hir1/Hir2 inter protein cross-links detected on SBD of Ssa1 and NLS of Hir1 and NTD of Hir2. (B) Ssa1-Hir1/2 cross links mapped on the crystal structure of Ssa1, Hir1 and Hir2. (C) Hir complex interacts with the chaperone complex. (D) Hir1 and Hir2 are destabilized in Ssa1-45 mutant strain. (E) HIRA complex interacts with chaperone complexes in mammalian cells. IP analysis of the HIRA complex in mammalian cells. (F) Western blot analysis of HIRA upon addition of Hsp70 inhibitor JG-98 and proteasomal inhibitor Bortezomib.

Figure 5. Pim1 phosphorylation regulates mitochondrial clearance in an Ssa1-dependent manner. (A) Schematic representation of Ssa1-Pim1 inter protein cross-links detected on NBD of Ssa1 and proteolytic domain of Pim1. (B) Ssa1-Pim1 cross links mapped on the crystal structure. (C) Pim1 interacts with the chaperone complex in yeast cells. (D) IP analysis of Lonp-1 interacts with chaperone complexes in mammalian cells. (E) Western blot analysis of Lonp-1 upon addition of Hsp70 inhibitor JG-98 and proteasomal inhibitor Bortezomib. (F) Growth assay of Pim1 phospho mutants in yeast. (G) Fluorescence images of cells expressing FlucSM–RFP and Tom70-GFP. Scale bars are 10 μM. (H) Western blot analysis of Pim1 wildtype and phosphomutants upon addition of Bortezomib. (I) IP analysis of Pim1 wildtype and phospho mutants with chaperone

complex. (J) Western Blot analysis of Pim1 (wildtype and phospho-mutants) expressed in the presence or absence of Ssa1 *in E.coli*. (K) Schematic of Ssa1 regulation of Pim1.

Figure 6. Mtw1 is a client of Hsp70 and is regulated by phosphorylation. (A) Schematic representation of Ssa1-Mtw1 inter protein cross-links detected on NBD of Ssa1 and head domain of Mtw1. (B) Ssa1-Mtw1 cross links mapped on the crystal structure of Ssa1 and Mtw1. (C) Mtw1 interacts with the chaperone complex. (D) Mtw1 is destabilized in Ssa1-45 mutant strain. (E) MIS12 interacts with chaperone complexes in mammalian cells. (F) Western blot analysis of MIS12 upon addition of Hsp70 inhibitor JG-98 and proteasomal inhibitor Bortezomib. (G) Growth assay analyzing the phenotype of the Mtw1 and its Y86 mutant. (H) Mtw1 was tagged with YFP in wild-type and Mtw1-Y86F mutant strains to compare Mtw1 localization at the kinetochore using Fluorescence microscopy. (I) Fluorescence intensities were quantified in wildtype and mutant Mtw1 using the semi-automated FociQuant ImageJ script (Ledesma-Fernandez and Thorpe, 2015). Intensities were compared using the Student's t-test (p-value=1.8E-12). (J) Analysis of the impact of Mtw1 phosphorylation on interaction with chaperones. (K) Model of Mtw1 activity regulation via its phosphorylation.

Figure 7. Ste11 dimethylation impacts the osmotic stress response. (A) Depiction of Ste11 pathway under hyperosmotic stress. (B) Schematic representation of Ssa1-Ste11 inter protein cross-links detected on NBD of Ssa1 and regulatory domain of Ste11. (C) Halo assay analyzing the phenotype of the Ste11 wildtype and methylation mutants in response to alpha factor. (D) FUS1-lacZ activity of Ste11 mutants in response to

pheromone. (E) Western blot analysis of the effect of Ste11 wildtype and mutants in response to pheromone signaling. (F) Growth assay analyzing the phenotype of the Ste11 wildtype and the methylation mutants in hyperosmotic stress. (G) 8xCRE lacZ activity of Ste11 mutants in response to osmotic stress. (H) Halo assay showing that none of the Ste11 variants permit pheromone response in the absence of Ste20. (I) IP analysis of Ste11 with chaperone complex. (J) Model of Ste11 activity regulation via its methylation.

Supplementary Figure S1 (A) Venn diagram representing previously known physical interactors of Ssa1 versus direct interactors of Ssa1 identified in this study. (B) Scatter plot of number of interactors identified versus surface lysine on the domains of Ssa1. (C) Bar graph representing interactors per cross linkable lysine on domains of Ssa1.

Supplementary Figure S2 (A). Localization of Pim1 wildtype and the mutants in yeast cells. (B) Quantification of percentage of cell with mitoFluc labeled DUMP structures in (Figure 5G). Paired t-test was used for statistical analysis. (C) Western blot showing the levels of Pim1 wildtype and the mutants in yeast cells.

Supplementary Figure 3 (A) Growth curves of wild-type (BY4741) and Mtw1-Y86F yeast strains. Cells were diluted from an overnight culture to OD_{600}=0.03 and the OD_{600} was measured every 5 minutes for 16 hours using a microplate reader. Growth analysis was performed in 10 replicates per strain. (B) Doubling times for wild-type and mutant strains were calculated for each replicate and compared using Student's t-test (mean=92.97 min, p-value=0.04).

Figure 1

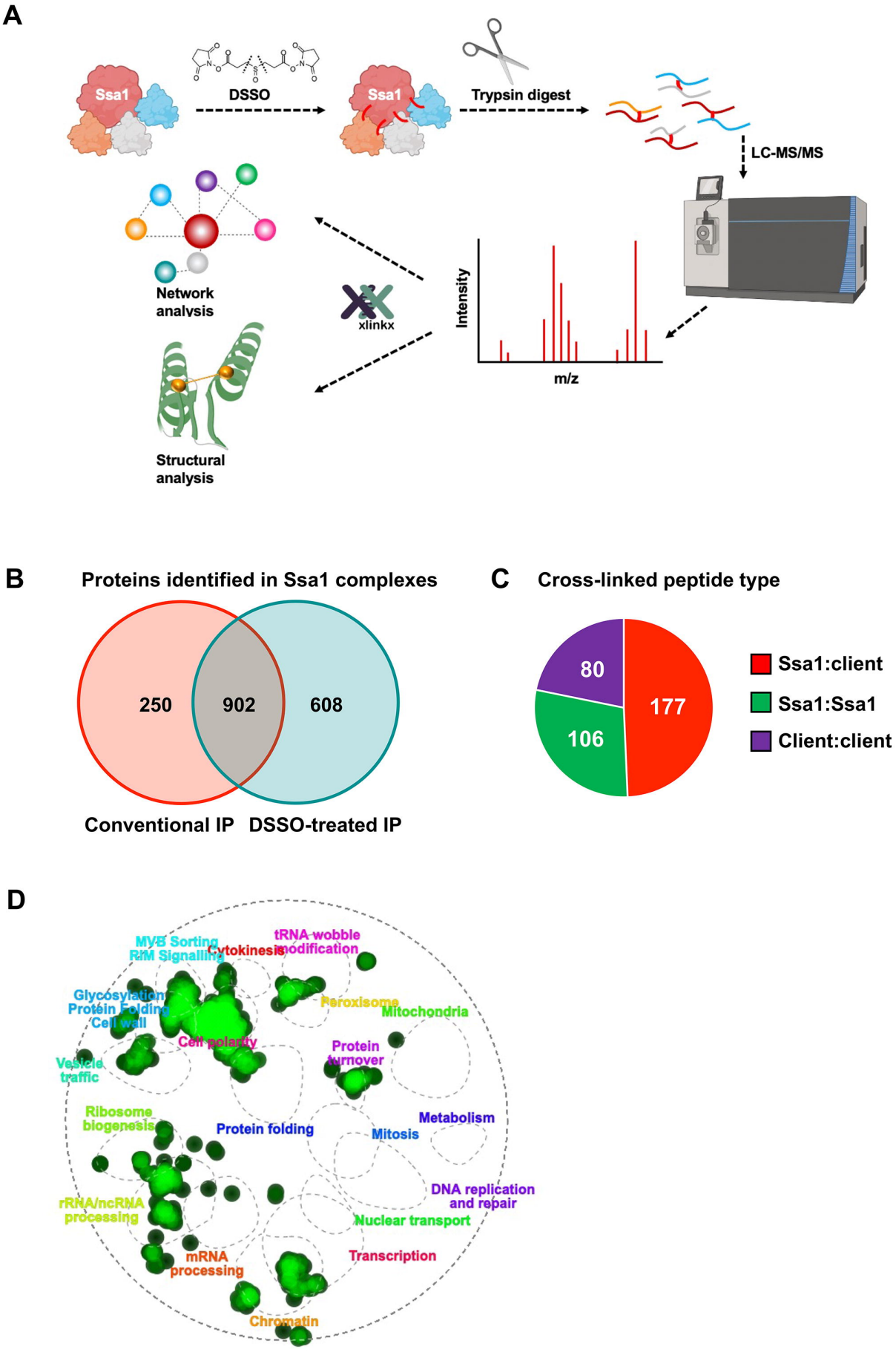
A
Ssa1
DSSO
Ssa1
Trypsin digest
LC-MS/MS
Network analysis
xlinkx
Intensity
m/z
Structural analysis
B
Proteins identified in Ssa1 complexes
250
902
608
Conventional IP
DSSO-treated IP
C
Cross-linked peptide type
80
177
106
Ssa1:client
Ssa1:Ssa1
Client:client
D
MVB Sorting
RIM Signalling
Cytokinesis
tRNA wobble modification
Glycosylation
Protein Folding
Cell wall
Peroxisome
Mitochondria
Cell polarity
Protein turnover
Vesicle traffic
Ribosome biogenesis
Protein folding
Metabolism
Mitosis
DNA replication and repair
rRNA/ncRNA processing
Nuclear transport
mRNA processing
Transcription
Chromatin

Figure 2

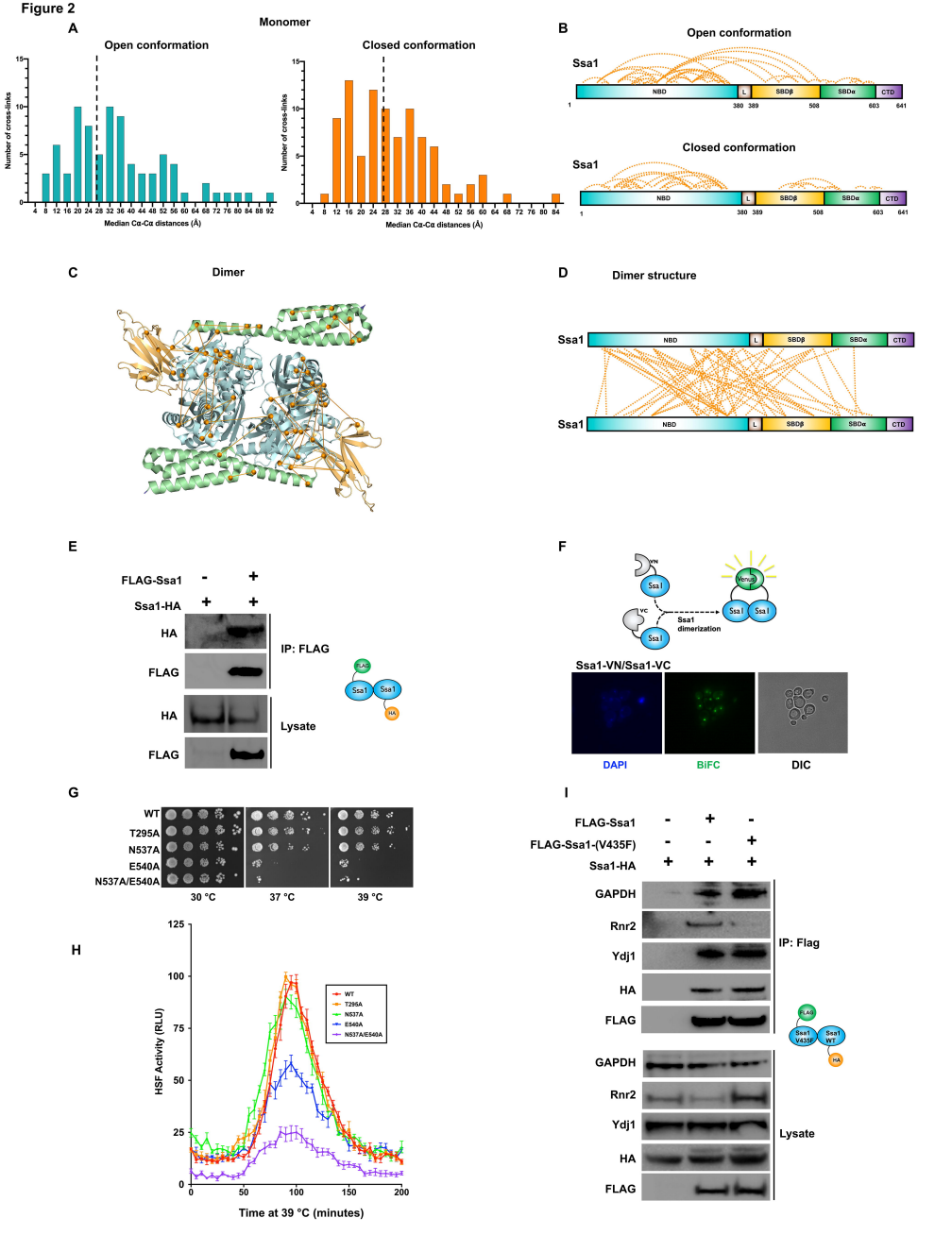
A
Monomer
Open conformation
Closed conformation
Number of cross-links
Median Cα-Cα distances (Å)
B
Open conformation
Closed conformation
Ssa1
NBD
L
SBDβ
SBDα
CTD
C
Dimer
D
Dimer structure
E
FLAG-Ssa1
Ssa1-HA
HA
FLAG
IP: FLAG
Lysate
F
VN
VC
Ssa1
Venus
Ssa1 dimerization
Ssa1-VN/Ssa1-VC
DAPI
BiFC
DIC
G
WT
T295A
N537A
E540A
N537A/E540A
30 °C
37 °C
39 °C
H
HSF Activity (RLU)
Time at 39 °C (minutes)
I
FLAG-Ssa1
FLAG-Ssa1-(V435F)
Ssa1-HA
GAPDH
Rnr2
Ydj1
HA
FLAG
IP: Flag
Lysate

Figure 3

A

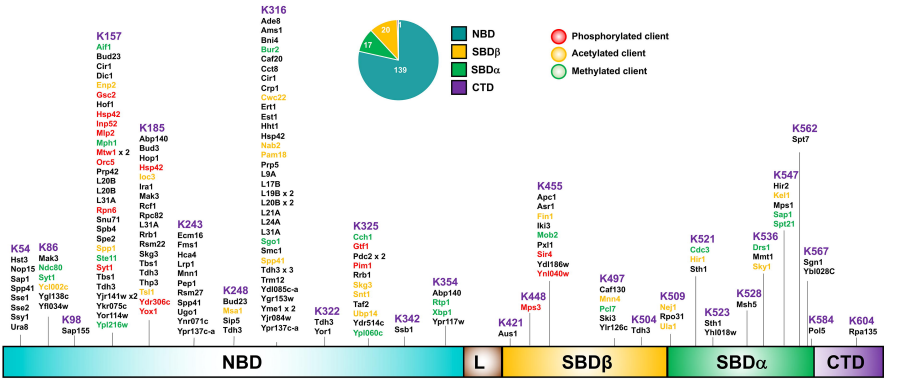
K157
Alf1
Bud23
Cir1
Dic1
Erp2
Gsc2
Hof1
Hsp42
Inp52
Mlp2
Mph1
Mtw1 x 2
Orc5
Prp42
L20B
L20B
L31A
Rpn6
Snu71
Spb4
Spe2
Spo7
Ste11
Syt1
Tbs1
Tdh3
Yjr141w x2
Ykr075c
Yor114w
Ypl216w
K185
Abp140
Bud3
Hop1
Hsp42
Ioc3
Ira1
Mak3
Rcf1
Rpc82
L31A
Rrb1
Rsm22
Skg3
Tbs1
Tdh3
Thp3
Tal1
Ydr306c
Yox1
K243
Ecm16
Fms1
Hca4
Lrp1
Mnn1
Pep1
Rsm27
Spp41
Ugo1
Ynr071c
Ypr137c-a
K316
Ade8
Ams1
Bni4
Bur2
Caf20
Cct8
Cir1
Crp1
Csc22
Ert1
Est1
Hht1
Hsp42
Nab2
Pam18
Prp5
L9A
L17B
L19B x 2
L20B x 2
L21A
L24A
L31A
Sgo1
Smc1
Spp41
Tdh3 x 3
Trm12
Ydl085c-a
Ygr153w
Yme1 x 2
Yjr084w
Ypr137c-a
K248
Bud23
Mph1
Sip5
Tdh3
K322
Tdh3
Yor1
K325
Cch1
Gtf1
Pdc2 x 2
Pim1
Rrb1
Skg3
Snt1
Taf2
Ubp14
Ydr514c
Ypl060c
K342
Ssb1
K354
Abp140
Rtp1
Xbp1
Ypr117w
K421
Aus1
K448
Mps3
K455
Apc1
Asr1
Fin1
Iki3
Mob2
Pxl1
Sir4
Ydl186w
Ynl040w
K497
Caf130
Mnn4
Pcf7
Ski3
Ylr126c
K504
Tdh3
K509
Nap1
Rpo31
Ula1
K521
Cdc3
Hir1
Sth1
K523
Sth1
Yhl018w
K528
Msh5
K536
Drs1
Mmt1
Sky1
K547
Hir2
Mps1
Sap1
Spt21
K562
Spt7
K567
Sgn1
Ybl028C
K54
Hst3
Nop15
Sap1
Spp41
Sse1
Sse2
Ssy1
Ura8
K86
Mak3
Ndc80
Syt1
Ydl002c
Ygl138c
Yfl034w
K98
Sap155
K584
Pol5
K604
Rpa135
NBD
L
SBDβ
SBDα
CTD
139
17
20
NBD
SBDβ
SBDα
CTD
Phosphorylated client
Acetylated client
Methylated client

B

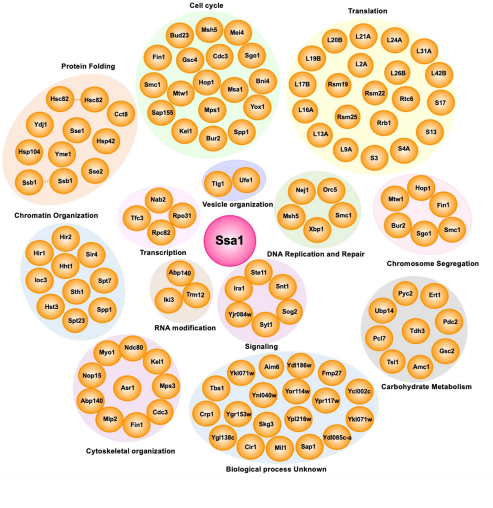
Cell cycle
Translation
Protein Folding
Chromatin Organization
Vesicle organization
Transcription
DNA Replication and Repair
Chromosome Segregation
Ssa1
RNA modification
Signaling
Carbohydrate Metabolism
Cytoskeletal organization
Biological process Unknown

C

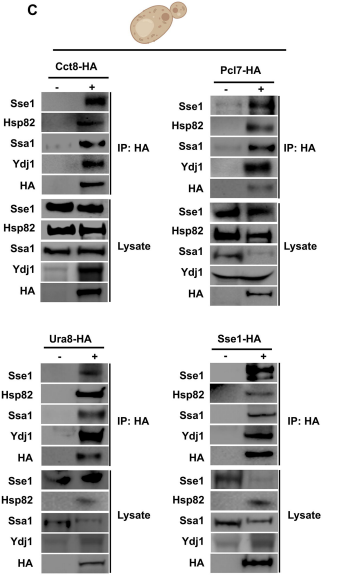
Cct8-HA
Pcl7-HA
Ura8-HA
Sse1-HA
-
+
Sse1
Hsp82
Ssa1
Ydj1
HA
IP: HA
Lysate

Figure 4

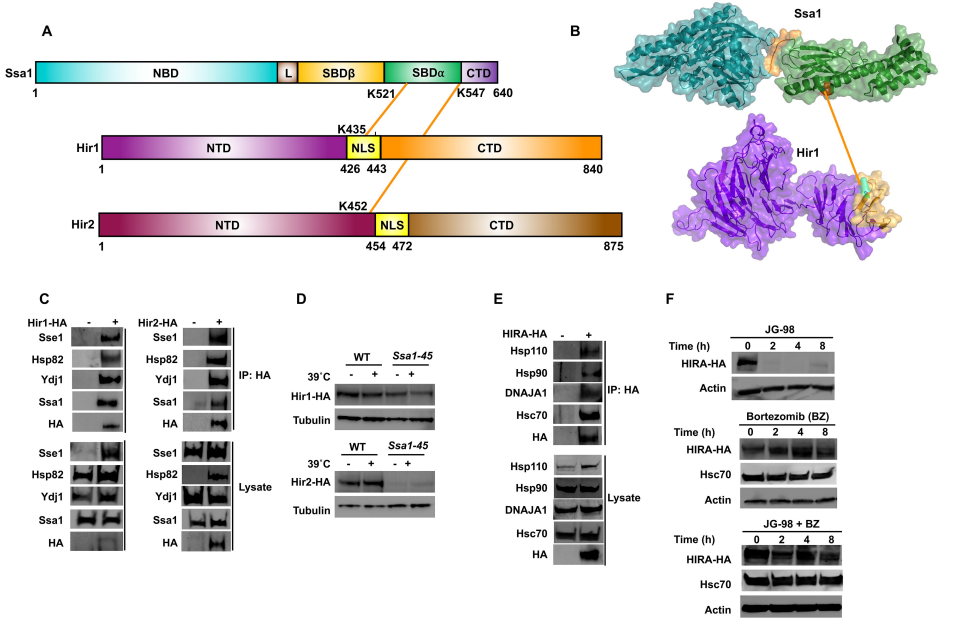
A
Ssa1
NBD
L
SBDβ
SBDα
CTD
1
K521
K547
640
K435
Hir1
NTD
NLS
CTD
1
426
443
840
K452
Hir2
NTD
NLS
CTD
1
454
472
875
B
Ssa1
Hir1
C
Hir1-HA
Hir2-HA
Sse1
Hsp82
Ydj1
Ssa1
HA
IP: HA
Lysate
D
WT
Ssa1-45
39°C
Hir1-HA
Hir2-HA
Tubulin
E
HIRA-HA
Hsp110
Hsp90
DNAJA1
Hsc70
HA
IP: HA
Lysate
F
JG-98
Bortezomib (BZ)
JG-98 + BZ
Time (h)
0
2
4
8
HIRA-HA
Hsc70
Actin

Figure 5

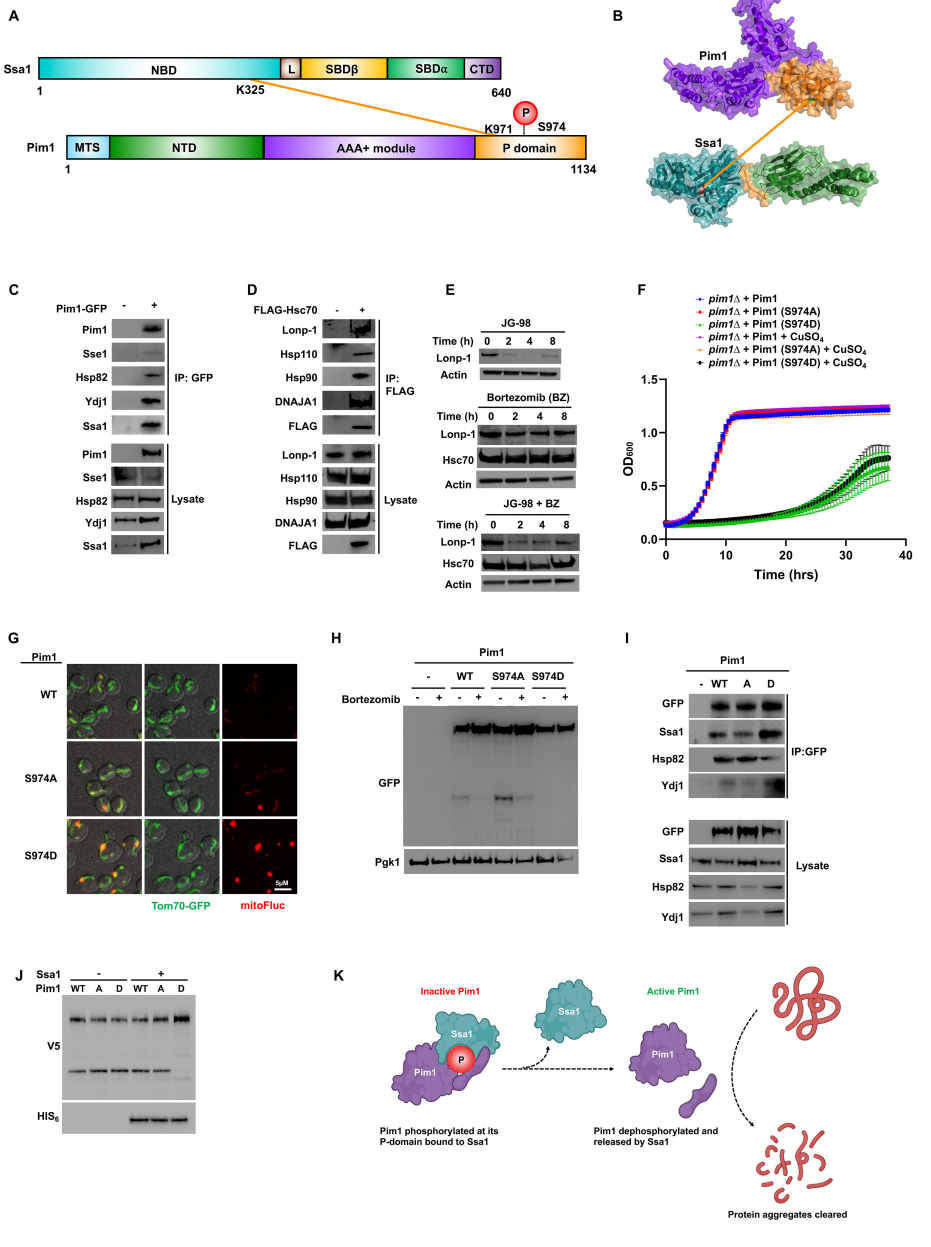
A
Ssa1
NBD
L
SBDβ
SBDα
CTD
1
K325
640
P
K971
S974
Pim1
MTS
NTD
AAA+ module
P domain
1
1134
B
Pim1
Ssa1
C
Pim1-GFP
-
+
Pim1
Sse1
Hsp82
Ydj1
Ssa1
IP: GFP
Pim1
Sse1
Hsp82
Ydj1
Ssa1
Lysate
D
FLAG-Hsc70
-
+
Lonp-1
Hsp110
Hsp90
DNAJA1
FLAG
IP: FLAG
Lonp-1
Hsp110
Hsp90
DNAJA1
FLAG
Lysate
E
JG-98
Time (h)
0
2
4
8
Lonp-1
Actin
Bortezomib (BZ)
Time (h)
0
2
4
8
Lonp-1
Hsc70
Actin
JG-98 + BZ
Time (h)
0
2
4
8
Lonp-1
Hsc70
Actin
F
pim1Δ + Pim1
pim1Δ + Pim1 (S974A)
pim1Δ + Pim1 (S974D)
pim1Δ + Pim1 + CuSO4
pim1Δ + Pim1 (S974A) + CuSO4
pim1Δ + Pim1 (S974D) + CuSO4
OD600
1.5
1.0
0.5
0.0
0
10
20
30
40
Time (hrs)
G
Pim1
WT
S974A
S974D
5μM
Tom70-GFP
mitoFluc
H
Pim1
-
WT
S974A
S974D
Bortezomib
-
+
-
+
-
+
-
+
GFP
Pgk1
I
Pim1
-
WT
A
D
GFP
Ssa1
Hsp82
Ydj1
IP:GFP
GFP
Ssa1
Hsp82
Ydj1
Lysate
J
Ssa1
-
+
Pim1
WT
A
D
WT
A
D
V5
HIS6
K
Inactive Pim1
Ssa1
P
Pim1
Active Pim1
Ssa1
Pim1
Pim1 phosphorylated at its P-domain bound to Ssa1
Pim1 dephosphorylated and released by Ssa1
Protein aggregates cleared

Figure 6

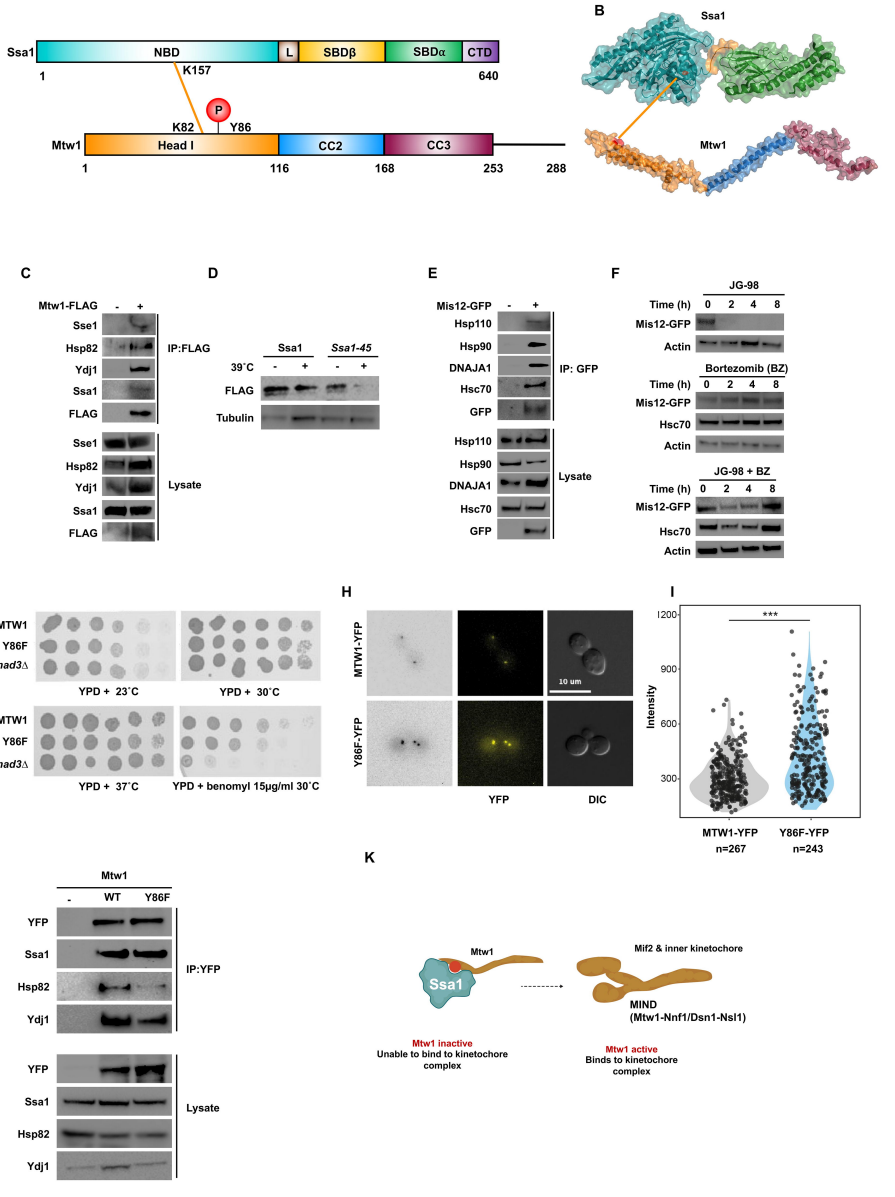
A
Ssa1
NBD
L
SBDβ
SBDα
CTD
1
K157
640
P
K82
Y86
Mtw1
Head I
CC2
CC3
1
116
168
253
288
B
Ssa1
Mtw1
C
Mtw1-FLAG
-
+
Sse1
Hsp82
Ydj1
Ssa1
FLAG
IP:FLAG
Sse1
Hsp82
Ydj1
Ssa1
FLAG
Lysate
D
Ssa1
Ssa1-45
39˚C
-
+
-
+
FLAG
Tubulin
E
Mis12-GFP
-
+
Hsp110
Hsp90
DNAJA1
Hsc70
GFP
IP: GFP
Hsp110
Hsp90
DNAJA1
Hsc70
GFP
Lysate
F
JG-98
Time (h)
0
2
4
8
Mis12-GFP
Actin
Bortezomib (BZ)
Time (h)
0
2
4
8
Mis12-GFP
Hsc70
Actin
JG-98 + BZ
Time (h)
0
2
4
8
Mis12-GFP
Hsc70
Actin
G
MTW1
Y86F
mad3Δ
YPD + 23˚C
YPD + 30˚C
MTW1
Y86F
mad3Δ
YPD + 37˚C
YPD + benomyl 15µg/ml 30˚C
H
MTW1-YFP
Y86F-YFP
10 um
YFP
DIC
I
***
1200
900
600
300
Intensity
MTW1-YFP
n=267
Y86F-YFP
n=243
J
Mtw1
-
WT
Y86F
YFP
Ssa1
Hsp82
Ydj1
IP:YFP
YFP
Ssa1
Hsp82
Ydj1
Lysate
K
Mtw1
Ssa1
Mif2 & inner kinetochore
MIND
(Mtw1-Nnf1/Dsn1-Nsl1)
Mtw1 inactive
Unable to bind to kinetochore complex
Mtw1 active
Binds to kinetochore complex

Figure 7

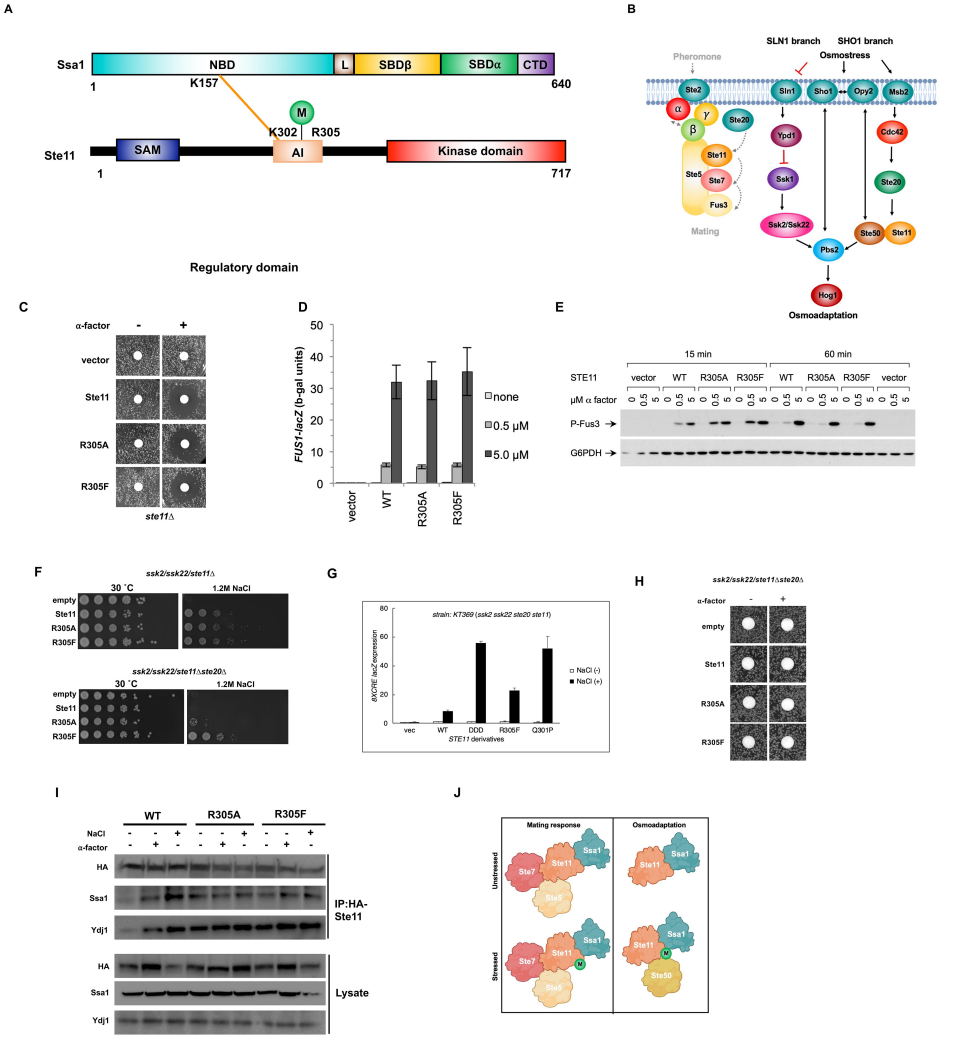
A
Ssa1
NBD
L
SBDβ
SBDα
CTD
1
K157
640
M
K302
R305
Ste11
SAM
AI
Kinase domain
1
717
Regulatory domain
B
SLN1 branch
SHO1 branch
Osmostress
Pheromone
Ste2
Sln1
Sho1
Opy2
Msb2
α
γ
β
Ste20
Ypd1
Cdc42
Ste11
Ste5
Ste7
Fus3
Ssk1
Ste20
Mating
Ssk2/Ssk22
Pbs2
Ste50
Ste11
Hog1
Osmoadaptation
C
α-factor
-
+
vector
Ste11
R305A
R305F
ste11Δ
D
FUS1-lacZ (b-gal units)
none
0.5 μM
5.0 μM
vector
WT
R305A
R305F
E
15 min
60 min
STE11
vector
WT
R305A
R305F
WT
R305A
R305F
vector
μM α factor
P-Fus3
G6PDH
F
ssk2/ssk22/ste11Δ
30 ˚C
1.2M NaCl
empty
Ste11
R305A
R305F
ssk2/ssk22/ste11Δste20Δ
30 ˚C
1.2M NaCl
empty
Ste11
R305A
R305F
G
strain: KT369 (ssk2 ssk22 ste20 ste11)
ΔXCRE lacZ expression
NaCl (-)
NaCl (+)
vec
WT
DDD
R305F
Q301P
STE11 derivatives
H
ssk2/ssk22/ste11Δste20Δ
α-factor
-
+
empty
Ste11
R305A
R305F
I
WT
R305A
R305F
NaCl
α-factor
HA
Ssa1
Ydj1
IP:HA-Ste11
HA
Ssa1
Ydj1
Lysate
J
Mating response
Osmoadaptation
Unstressed
Stressed
Ssa1
Ste11
Ste7
Ste5
M
Ste50

Supplementary figures

A

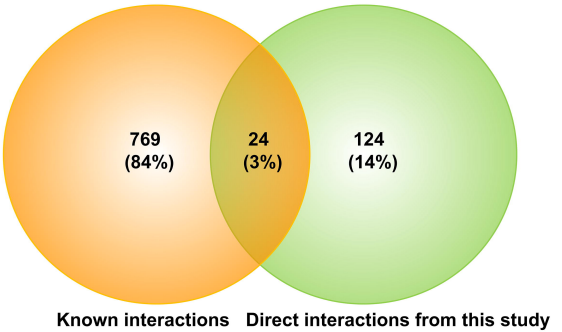

B

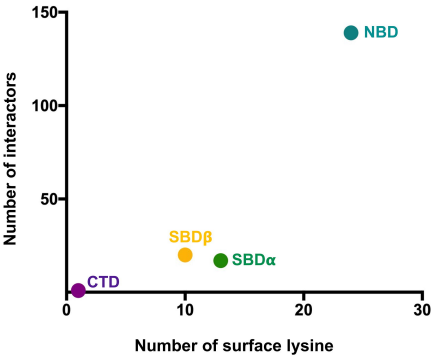

C

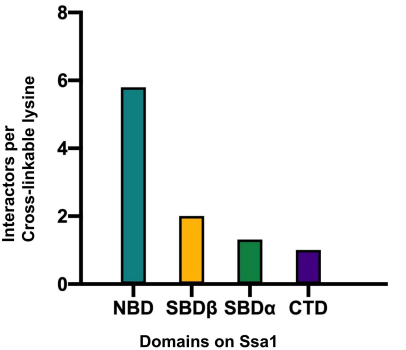

S2

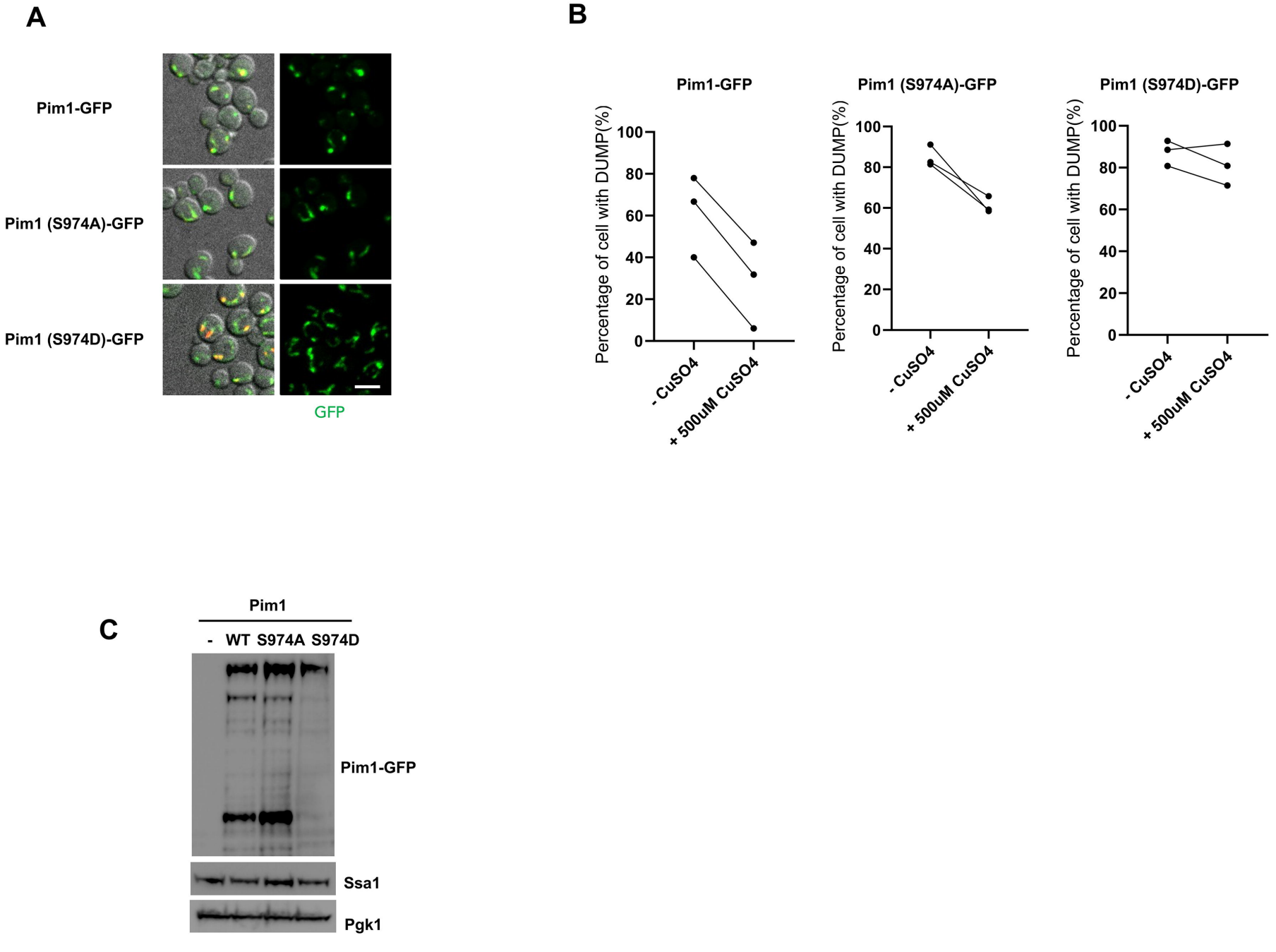
A
Pim1-GFP
Pim1 (S974A)-GFP
Pim1 (S974D)-GFP
GFP
B
Pim1-GFP
Pim1 (S974A)-GFP
Pim1 (S974D)-GFP
Percentage of cell with DUMP(%)
100
80
60
40
20
0
- CuSO4
+ 500uM CuSO4
C
Pim1
- WT S974A S974D
Pim1-GFP
Ssa1
Pgk1

S3

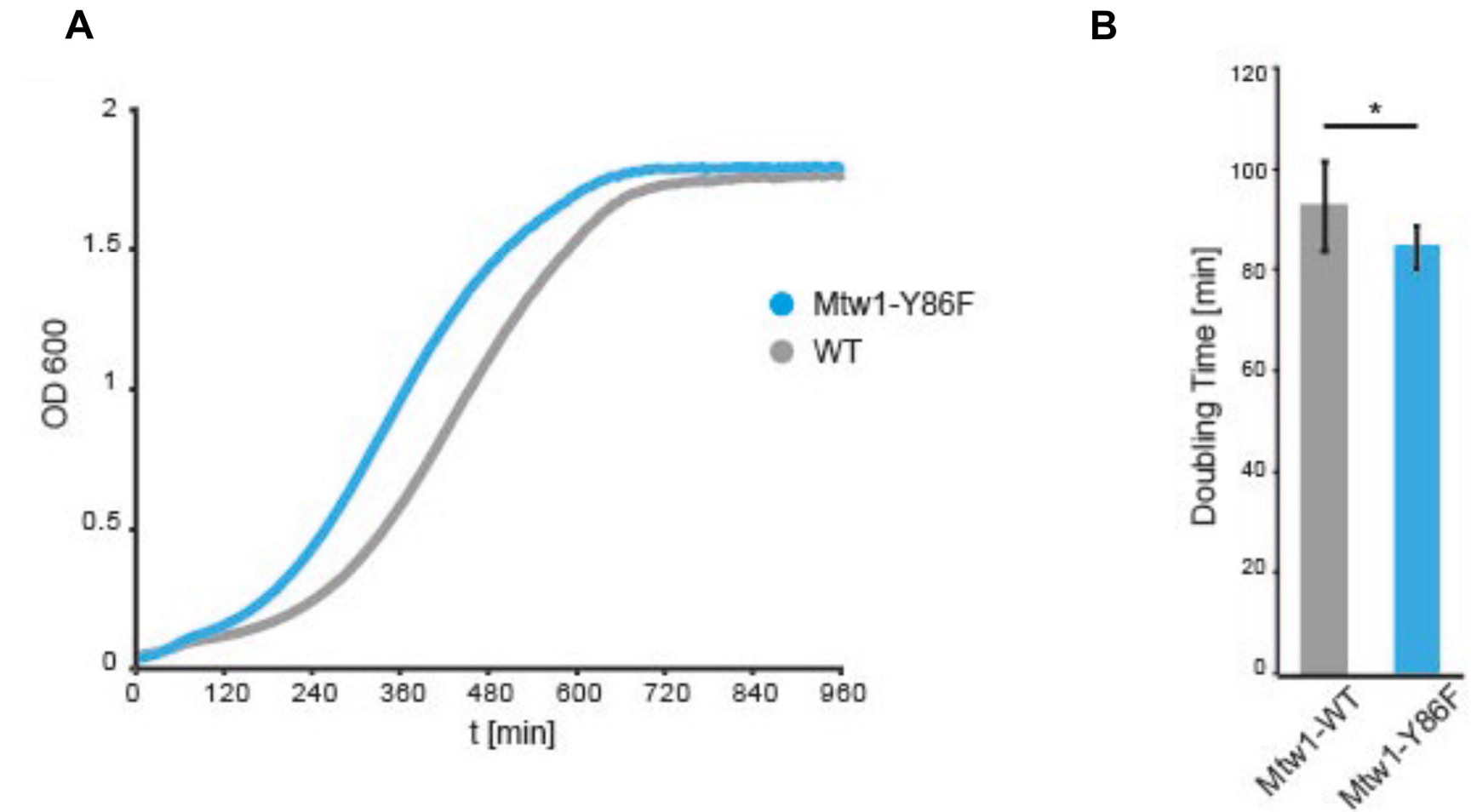
A
OD 600
2
1.5
1
0.5
0
0
120
240
360
480
600
720
840
960
t [min]
Mtw1-Y86F
WT
B
Doubling Time [min]
120
100
80
60
40
20
0
*
Mtw1-WT
Mtw1-Y86F